Journal of Applied Fluid Mechanics, Vol. 16, No. 11, pp. 2115-2129, 2023.
Available online at www.jafmonline.net, ISSN 1735-3572, EISSN 1735-3645.
https://doi.org/10.47176/jafm.16.11.1931

A Unified Transformation Framework for Studying Various Situations of Vertical/Oblique Drop Impact on Horizontal/Inclined Stationary/Moving Flat Surfaces

E. Azadi and M. Taeibi Rahni†

Department of Aerospace Engineering, Sharif University of Technology, Tehran, 11155-9161, Iran

†*Corresponding Author Email: taeibi@sharif.edu*

ABSTRACT

There are various situations of drop impact on solid surfaces widely occurred in natural phenomenon or used in different industrial applications. However, comparing and classifying these drop impact situations is not easy due to different states of the parameters affecting drop impact dynamics. In this article, a unified transformation framework is proposed to study various situations of vertical/oblique drop impact on horizontal/inclined stationary/moving flat surfaces with/without a crossflow. This simple framework consists of a coordinate with normal and tangential axes on a horizontal stationary surface. For each drop impact situation, the drop velocity, gravitational acceleration, possible induced flow due to the moving surface, and possible crossflow are transformed into the framework. Comparing the transformed versions of considered drop impact situations facilitates identification of their physical similarities/differences and determines which situations (and under what conditions) lead to identical results and can be used interchangeably. Although common situations of drop impact on moving surfaces (having tangential component of surface velocity) lead to asymmetric drop spreading, the possibility of symmetric drop spreading on moving surfaces is demonstrated and analyzed using the proposed transformation framework. This interesting possibility means that for related production lines or experimental setups, where symmetrical drop spreading is required, the surface does not need to be stationary. In such applications/setups, the use of moving surfaces (rather than stationary surfaces) can considerably accelerate the symmetric drop impact process. Our simulation results of several of the considered drop impact situations well confirm the facilities/predictions of the proposed transformation framework.

Article History

Received April 12, 2023
Revised June 22, 2023
Accepted July 3, 2023
Available online September 3, 2023

Keywords:

Drop impact on flat surfaces
Symmetric drop spreading on moving surfaces
Unified transformation framework
Accelerating drop impact process
Fast production lines

1. INTRODUCTION

Drop impact on solid surfaces is a widespread phenomenon in nature and industry. Typical examples include raindrop erosion, inkjet printing, fuel spraying, coating, painting, aircraft deicing, surface cooling, and self-cleaning surfaces (Moreira et al., 2010; Marengo et al., 2011; Josserand & Thoroddsen, 2016). This phenomenon is also widely used in thermal systems, thermal spraying, and surface cooling due to its high heat transfer capacity (Benther et al., 2021; Xu et al., 2022; Dai et al., 2023). The importance of understanding and controlling drop-surface interaction in various situations is growing due to advances in additive manufacturing, interfacial materials, microfluidic devices, medical applications, and electronic boards/devices (Mohammad Karim, 2023; Wang et al., 2022). In addition, the dynamic contact line and the surface wettability topics are related to drop-solid investigations (Marengo et al., 2011). Interactions between forces such as inertial, viscous, interfacial, aerodynamic, and gravity cause the dynamics of drop impact on surfaces (Mohammad Karim, 2023).

In the phenomenon of drop impact on a flat surface, the drop velocity can be vertical/oblique, the surface can be horizontal/inclined and stationary/moving, and a crossflow may or may not be present. These differences lead to various drop impact situations having different physical and technical properties. Most studies have been

NOMENCLATURE

Parameters

A	constant related to chemical potential
c_s	speed of sound
dV	cell volume
D_0	initial drop diameter
DW	downstream drop spreading width
DW^*	dimensionless downstream drop spreading width
e_n	normal component of unit vector
e_t	tangential component of unit vector
$\vec{F}_b$	body force vector
Fr_n	Froude number
$\vec{F}_s$	surface tension force vector
g	gravitational acceleration
g_n	normal componnet of gravitational acceleration
g_t	tangential componnet of gravitational acceleration
H	drop spreading height
H^*	dimensionless drop spreading height
H_{eq}	drop equilibrium height
H^*_{eq}	dimensionless equilibrium height
k	constant related to interface curvature
m_g^0	mass of gas phase at $t = t^0$
m_g^n	mass of gas phase at $t = t^n$
M	constant mobility
$\vec{n}$	surface unit normal vector
L_0	boundary layer length characteristic
L_x	domain length in x direction
L_y	domain length in y direction
p	pressure
q	source term used for conservation of mass
$\vec{r}$	location vector
$\vec{r}_c$	location vector of drop center
Re_n	Reynolds number
Re_{L_0}	Reynolds number of the boundary layer flow
t	time
T	dimensionless time
$\vec{u}$	flow velocity vector
$u_{x,bl}$	boundary layer velocity
UW	upstream drop spreading width
UW^*	dimensionless upstream drop spreading width
V_d	drop impact velocity
V_{dn}	normal component of drop impact velocity
V_{dt}	tangential component of drop impact velocity
$V_{g,fs}$	gas free-stream velocity
$V_{g,w}$	gas flow velocity just above the surface
V_s	surface velocity
W	drop spreading width
W^*	dimensionless drop spreading width
We_n	Weber number
W_{eq}	drop equilibrium width
W^*_{eq}	dimensionless drop equilibrium width

Greek symbols

α	inclination angle of surface
β	angle of surface velocity
δ	boundary layer thickness
Δt	time step
ΔV	volume of interfacial region
θ	oblique angle of drop velocity
θ_c	contact angle
μ	dynamical viscosity
μ_g	gas dynamical viscosity
μ_l	liquid dynamical viscosity
μ_ϕ	chemical potential
ξ	interface thickness
ρ	density
ρ_g	gas density
ρ_l	liquid density
σ	surface tension coefficient
ϕ	order parameter
Ω_g	gas phase region

Abbreviations

2D	two-dimensional
3D	three-dimensional
CH	Cahn-Hilliard
MLBFS	multiphase lattice Boltzmann flux solver
NS	Navier-Stokes

focused on the dynamics of the simplest situation i.e., vertical drop impact on horizontal stationary surfaces (Pasandideh-Fard et al., 1996, 1998; Rioboo et al., 2001; Xu et al., 2005; Xu, 2007; Marengo et al., 2011; Josserand & Thoroddsen, 2016; Gordillo et al., 2019). In the last two decades however, a number of investigations have been conducted on understanding the dynamics of more complex situations: oblique drop impact on horizontal stationary surfaces (Yin et al., 2018; Shusheng et al., 2020; Zhao et al., 2022), drop impact on inclined stationary surfaces(Šikalo et al., 2005; Lunkad et al., 2007; Cui et al., 2009; Antonini et al., 2014; LeClear et al., 2016; Shen et al., 2016; Zhang et al., 2017; Hao et al., 2019; Jiang & Zhou, 2020; Sahoo et al., 2020), drop impact on moving surfaces(Chen & Wang, 2005; Fathi et al., 2010; Almohammadi & Amirfazli, 2017a, 2017b; Hao & Green, 2017; Buksh et al., 2019; Zhan et al., 2021), and drop impact on horizontal stationary surfaces including a gas crossflow (Cunha et al., 2018; Ferrao et al., 2019; Ferrao et al., 2020; Pereira, 2019). The latter situations are more common in natural phenomena and practical applications (Almohammadi & Amirfazli, 2017a; García-Geijo et al., 2020). In the following, the physical aspects and the investigations carried out to compare and combine these situations (more complex ones) are reviewed.

In the above drop impact situations having tangential (relative to the surface) component of drop impact velocity, the drop inertial force has a component tangential to the surface as well. Such a force leads to asymmetric drop spreading/splashing on the surface. For the drop impact situations with inclined surfaces, the gravity force has also a component tangential to the surface. The possible moving surface induces a boundary layer flow above the surface which can affect the drop dynamics within the boundary layer (Almohammadi & Amirfazli, 2017a, b). The possible crossflow inserts aerodynamic forces on the drop both outside and inside the boundary layer (Ferrao et al., 2019, 2020).

According to the authors' research, no studies have compared the aforementioned drop impact situations altogether. However, there are a few studies in the literature that have made a comparison between two of them. Note that, if the drop impact results of two of these situations are similar, their results (and even their experimental setups) can be used interchangeably. Bird et al. (Bird et al., 2009) experimentally studied two situations of drop impact on inclined surfaces (with inclination angle from 0 to 50° with respect to a horizontal plane) and drop impact on moving surfaces (with tangential velocity from 0 to 21 m/s). For the given normal and tangential drop impact velocities of millimeter-sized drops, they reported similar results for both cases. Buksh et al. (Buksh et al., 2020) reported that the experimental results of drop impact on horizontal moving surfaces having tangential velocity and drop impact on inclined surfaces are similar, where these cases have the same normal and tangential drop impact velocities. They concluded that both situations are equivalent (Buksh et al., 2020). García-Geijo et al. (García-Geijo et al., 2020) developed an analytical model (assuming negligible gravity effects) to predict asymmetric spreading of drops on stationary/moving surfaces for situations where the tangential drop impact velocity is present. Ferrao et al. (Ferrao et al., 2019) experimentally studied the drop impact on an inclined surface and drop impact on a horizontal surface including a crossflow, where in the latter case the crossflow causes the drop to impact the surface obliquely. They observed that for the same drop impact velocities, the results of these two situations are not identical (due to the drop deformation caused by the aerodynamic forces related to the crossflow).

In addition to the mentioned studies, there are a few articles in the literature combining the different situations of drop impact on flat surfaces. The combined situations of drop impact provide interesting opportunities for experimental setups and practical applications (e.g., achieving high-speed drop impact, decoupling normal and tangential drop impact velocities, controlling drop spreading/splashing results). Zen et al. (Zen et al., 2010) conducted an experiment to investigate the dynamics of drop impact on an inclined moving surface having tangential velocity. They observed that when the inclined surface moved downward with a special velocity, the drop impact results altered from downward splashing to surface deposition. Li (Li, 2013) developed an experimental setup to access and study the high-speed micron-sized drop impact on inclined moving surfaces having horizontal velocities of 10 to 63 m/s and inclination angles of 0 to 75° (with respect to a horizontal plane). Aboud and Kietzig (Aboud & Kietzig, 2015) investigated the dynamics of drop impact on inclined surfaces having horizontal velocities. The use of moving surfaces allowed them to examine the high-speed drop impact (up to 27 m/s) on inclined surfaces. Cimpeanu and Papageorgiou (Cimpeanu & Papageorgiou, 2018) simulated oblique drop impact (including a background air flow with the same oblique velocity) on a horizontal surface. Raman (Raman, 2019) simulated oblique drop impact on a horizontal moving surface, where the tangential component of oblique drop velocity is in the direction of surface velocity or in the opposite direction.

According to the reviewed studies, the parameters affecting the dynamics of drop impact on flat surfaces have different conditions leading to various situations of drop impact. However, there is hardly any work in which all the mentioned drop impact situations are systematically compared and classified. It seems the most important reason for this lack is that there is no unified framework for comparing and classifying these different situations.

In this article, a unified and simple transformation framework is proposed to study various situations of vertical/oblique drop impact on horizontal/inclined stationary/moving flat surfaces with/without a crossflow. For each situation, the parameters affecting drop impact dynamics are transformed into the framework. The resulting drop impact situation is called the transformed version. Comparing the transformed versions facilitates understanding their physical similarities/differences and determines which situations (and under what conditions) lead to identical results and can be used interchangeably. Also, for each case, technical possibilities/limitations for designing the related experimental setups and practical applications are discussed. In addition, possible combinations of the considered drop impact situations are presented and analyzed using the transformation framework. Note that, common situations of drop impact on moving surfaces (having tangential component of surface velocity) lead to asymmetric drop spreading. In this article however, for the first time the possibility of symmetric drop spreading on moving surfaces is demonstrated using the proposed framework. For this, three combined situations of drop impact on moving surfaces under special conditions -which can lead to symmetric drop spreading- are recognized and analyzed. Changing the target stationary surfaces with the proposed moving surfaces -whilst maintaining symmetric drop spreading- gives new opportunities and leads to faster operating drop impact processes in related fast production lines and experimental setups. Finally, several of the considered drop impact situations are numerically simulated, where the results confirm the facilitates and predictions of the proposed transformation framework.

The rest of this article is organized as follows. In section 02**,** first the unified transformation framework is introduced. Then, the basic situations of drop impact and their transformed versions are presented. Next, by comparing and classifying these transformed versions, the physical similarities/differences and technical possibilities/limitations of the considered drop impact situations are determined. In section 3, possible combinations (and their transformed versions) of the basic drop impact situations are covered. In section 4, the possibility of symmetric drop spreading on moving surfaces is introduced and discussed. In section 5, several of the considered drop impact situations are simulated and their results are analyzed. Finally, in section 6, the summaries and conclusions of this study are presented.

2. BASIC SITUATIONS AND THEIR TRANSFORMED VERSIONS

Before studying various situations of drop impact, it is appropriate here to explain the key terms used in this study for presenting these situations, as: vertical: in the direction of gravitational acceleration; oblique: the drop velocity has an angle with the vertical direction; inclined: the surface has an angle with a horizontal plane; normal/tangential: relative to the surface. In addition, the following symbols were used: V_d: drop velocity; g: gravitational acceleration; V_s: surface velocity; $V_{g,w}$: gas flow velocity on the surface; $V_{g,fs}$: gas free-stream flow velocity; and δ: boundary layer thickness.

The basic situations of dop impact on surfaces are presented in Table 1 (real cases). To facilitate analyzing, comparing, and classifying these different situations, a unified transformation framework is developed. This framework consists of a coordinate with normal and tangential axes on a horizontal stationary surface. For each real case, all effective parameters (i.e., the drop impact velocity, gravitational acceleration, possible induced flow due to the moving surface, and possible crossflow) are transformed to this framework to create the corresponding transformed version, see Table 1 (transformed versions).

2.1 Descriptions

The simplest possible situation of drop impact on a surface is vertical drop impact on a horizontal stationary surface (case B1). In this case, there are only the normal components of drop impact velocity and gravitational acceleration, therefore, the drop spreads/splashes symmetrically on the surface. In the oblique drop impact on a horizontal stationary surface (case B2), the existence of tangential component of drop impact velocity leads to asymmetric drop spreading/splashing on the surface.

Table 1 Schematics of basic situations of drop impact on flat surfaces and their transformed versions

Case	Real	Transformed
B1: Vertical Drop Impact on a Horizontal Stationary Surface	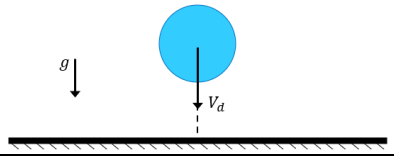	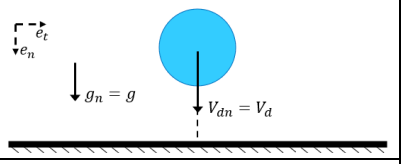
B2: Oblique Drop Impact on a Horizontal Stationary Surface	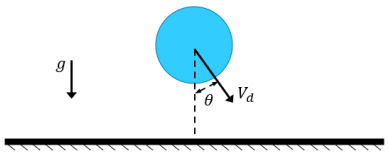	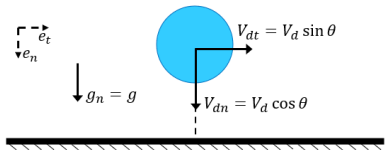
B3: Vertical Drop Impact on an Inclined Stationary Surface	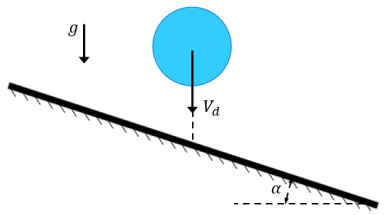	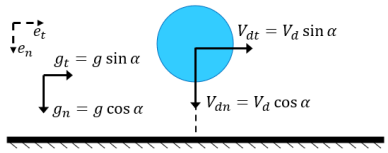
B4: Vertical Drop Impact on a Horizontal Moving Surface with Normal Velocity	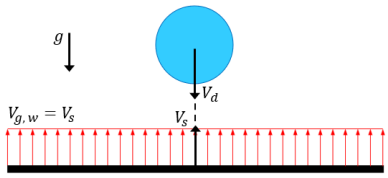	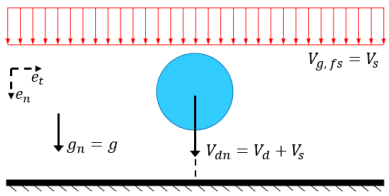
B5: Vertical Drop Impact on a Horizontal Moving Surface with Tangential Velocity	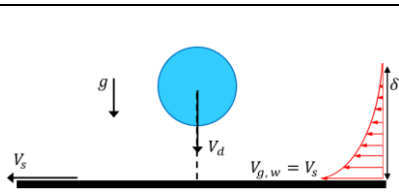	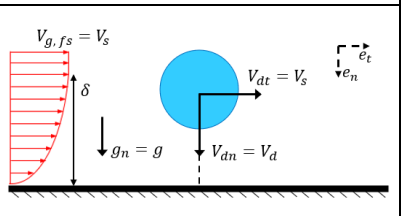
B6: Oblique Drop Impact on a Horizontal Stationary Surface with a Crossflow	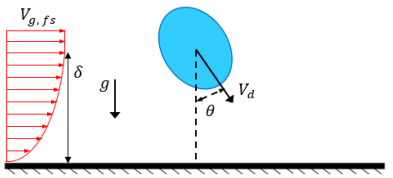	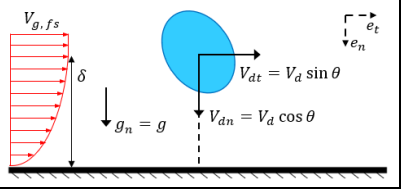

In case B3, drop impacts vertically on an inclined stationary surface. As shown in its transformed version, there are the normal and tangential components of both drop impact velocity and gravitational acceleration. Therefore, the drop has more tendency to spread/splash asymmetrically on the surface (compared to case B2).

In case B4, the drop impacts vertically on a horizontal moving surface having an upward velocity. This moving surface creates a flow field above the surface. In its transformed version, the surface velocity of the real case is added to the drop velocity and a free-stream downward flow is regarded. In this case, since both the drop impact velocity and gravity acceleration have no tangential component and the free-stream flow is in normal direction, the drop spreads/splashes symmetrically.

The vertical drop impact on a horizontal moving surface having a tangential velocity is considered in case B5. This moving surface creates a boundary layer flow above the surface. The flow velocity starts from the surface velocity and reaches zero at the top of the boundary layer. In its transformed version, the tangential component of drop impact velocity is equal to the surface velocity of the real case but in opposite direction, which leads to asymmetric drop spreading/splashing. Also, the flow velocity starts from zero to the free-stream velocity. Note that the free-stream flow does not affect the drop outside the boundary layer, because they have the same tangential velocity there. Note that, for typical surface velocities used in the related experimental setups and practical applications, the boundary layer thickness is often small enough for the drop velocity direction not to be affected by the flow. However, if the surface velocity is high, e.g., more than about 63 m/s for micron-sized drops (Li, 2013), the boundary layer flow pushes the drop away from the surface.

Finally in case B6, a falling drop influenced by a crossflow deforms and impacts a horizontal stationary surface obliquely. The crossflow affects the drop mainly outside the boundary layer. When a falling drop is influenced by a crossflow, it deviates from its initial path and deforms due to the exerted aerodynamic forces (Ferrao et al., 2019, 2020). The drop deformation and its oblique velocity cause asymmetric drop spreading/splashing on the surface. If the crossflow velocity exceeds a certain limit, the deformation of drop intensifies and finally the drop breakups before impacting the surfac (Ferrao et al., 2020; Carrolo et al., 2019).

2.2 Comparisons

Regarding the real cases in Table 1, the physics of each case is somehow different from the others. However, by comparing the transformed versions one can easily find their similarities/differences based on the drop impact velocity components, gravitational acceleration, possible flows caused by moving surfaces, and possible crossflow.

Comparing real cases in Table 1, only in cases B2 and B6 the drop velocity is oblique. Although a falling drop with an oblique velocity is common in nature, accessing a precise oblique drop velocity angle is not technically easy in practice. Note that, a falling drop with oblique velocity can be created in several ways, such as: lateral movement of a dripper nozzle, pressurized oblique nozzle, electrically charged falling drop, and falling drop in the vicinity of a crossflow. Obviously, such ways require more equipment and computations compared to creation of a falling drop with vertical velocity.

Comparing transformed cases in Table 1, only in cases B1 and B4 the parameters affecting drop impact dynamics do not have tangential components. In these cases, the drop spreads/splashes symmetrically on the surface. In case B4 the downward free-stream flow can make the drop impact results different from case B1 (despite having the same normal drop impact velocities). Note that, if the free-stream velocity is low, its effects are negligible and thus the results of both cases are almost the same. However, for this case further investigations are needed to determine the quantitative conditions leading to such negligible effects. On the other hand, since the drop terminal velocity is limited due to the exerted drag aerodynamic force (Aboud & Kietzig, 2015), case B1 cannot be used for the experimental testing of high-speed normal drop impact on surfaces (Li, 2013). In case B4 however, by increasing the upward surface velocity, accessing such high-speed normal drop impact can be possible in experiments.

Cases B2, B3, B5, and B6 (which have the tangential drop impact velocity in their transformed versions) occur extensively in natural phenomena and industrial applications. In addition to this tangential velocity, there is the tangential component of gravitational acceleration in case B3, the tangential boundary layer flow in case B5, and the tangential crossflow in case B6. All these tangential parameters can lead to asymmetric drop spreading/splashing and may cause the drop to slide on the surface (Aboud & Kietzig, 2018). Note that, in case B6, the inserted aerodynamic forces due to the crossflow often deform the drop before it impacts the surface. This deformation leads to different spreading/splashing results compared to impacting a spherical drop on the surface with the same drop impact velocity (Ferrao et al., 2019).

Comparing cases B2, B3, and B5, where they have the same V_{dn} as well as the same V_{dt}. If the gravity effects are negligible, cases B2 and B3 yield almost identical drop impact results. Also, if the boundary layer flow effects are negligible, cases B2 and B5 yield almost identical drop impact results. Consequently, if the effects of gravity and boundary layer flow are negligible, cases B2, B3, and B5 yield almost identical drop impact results. Note that, if such conditions (negligibility of such effects) are possible for two of these cases, then the available results (and even the setup) of one of them can be used instead of the other (due to the same results). The experimental studies of (Bird et al., 2009) and (Buksh et al., 2020) demonstrated the same drop spreading/splashing results for the vertical drop impact on inclined surfaces (case B3) and moving surfaces (case B5), where these cases have the same V_{dn} and V_{dt}. In both these experiments millimeter-sized drops were used. Buksh et al. (Buksh et al., 2020) noted that the gravity in case B3 and the boundary layer flow in case B5 did not affect initial drop spreading/splashing on surfaces, within the range of parameters used in their experiment.

Case B5 has two interesting and practical features compared to cases B2 and B3. First, the normal and tangential drop impact velocities in case B5 are independent since the tangential velocity is only related to the surface velocity. This allows an easier access to a wide range of tangential drop impact velocity in experimental setups and practical applications (despite keeping the normal drop impact velocity constant). Second, as mentioned before, since the drop terminal velocity is limited due to the drag force, cases B2 and B3 cannot be used to achieve high-speed tangential drop impact velocities. While the setup of case B5 allows such a high-speed tangential drop impact velocity by increasing the surface velocity. However, it is necessary to consider the effects of induced boundary layer flow.

Although the transformed versions of cases B5 and B6 have similar boundary layer flows, their results are dissimilar due to two main differences. In case B5, outside the boundary layer, the drop is not affected by the flow, therefore its path and shape do not change there (Almohammadi & Amirfazli, 2017a). While in case B6, the drop is deviated and deformed due to the exerted crossflow outside the boundary layer (Cunha et al., 2018).

3. COMBINED SITUATIONS AND THEIR TRANSFORMED VERSIONS

In this section, the drop impact situations resulting from the combinations of the considered basic cases in the previous section are presented, see Table 2.

Table 2 Schematics of combined situations of drop impact on flat surfaces and their transformed versions

Case	Real	Transformed
C1: Oblique Drop Impact on an Inclined Moving Surface with Velocity in an Arbitrary Direction	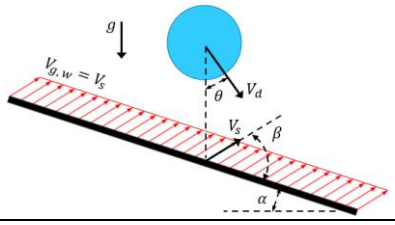	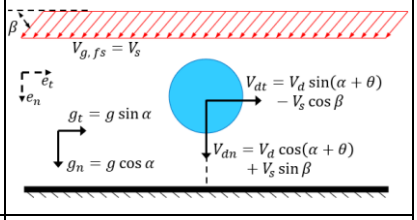
C2: Oblique Drop Impact on an Inclined Stationary Surface	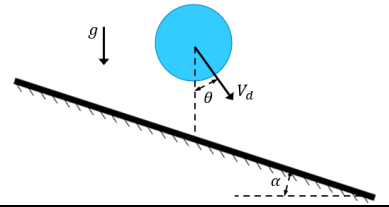	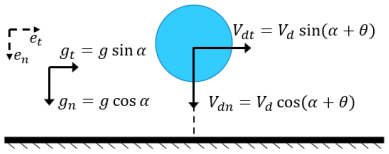
C3: Oblique Drop Impact on a Horizontal Moving Surface with Tangential Velocity	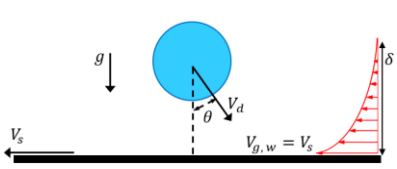	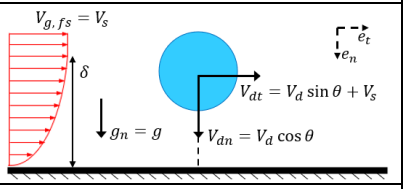
C4: Vertical Drop Impact on an Inclined Moving Surface with Tangential Velocity	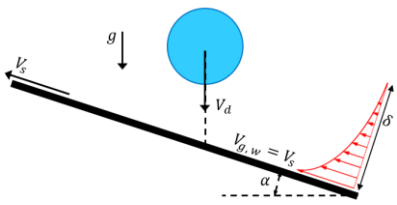	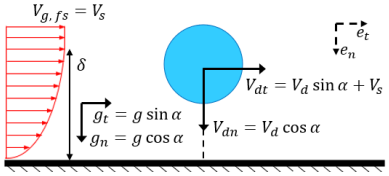
C5: Vertical Drop Impact on an Inclined Moving Surface with Horizontal Velocity	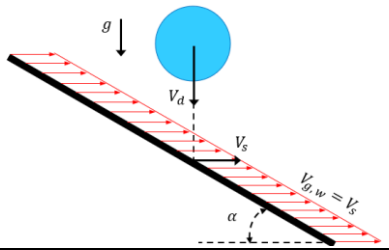	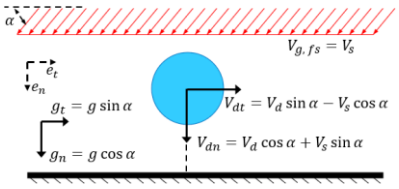
C6: Vertical Drop Impact on an Inclined Moving Surface with Vertical Velocity	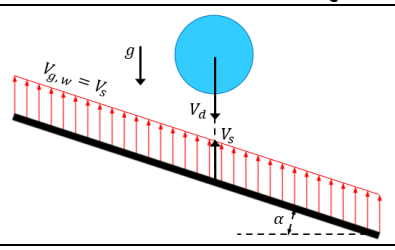	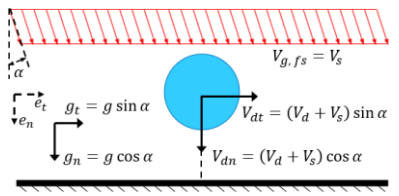

Case C1 presents a general combined case described as oblique drop impact on an inclined moving surface having velocity in an arbitrary direction. All possible combined cases of vertical/oblique drop impact on horizontal/inclined stationary/moving surfaces are special cases derived from this case. Other combined cases introduced in Table 2 are those which are more common in natural phenomena or have suitable features for designing experimental setups and practical applications. Some of these combined cases have previously been used for drop impact investigations: case C3 numerically by (Raman, 2019), case C4 experimentally by (Zen et al., 2010), case C5 experimentally by (Aboud & Kietzig, 2015) and (Li, 2013), and the transformed version of case C6 (with the difference that the gravity was normal to the surface) numerically by (Cimpeanu & Papageorgiou, 2018).

Note that, if the effects of the induced flows and gravity are negligible, then the transformed versions of these complex cases are simplified to the cases of oblique drop impact on horizontal stationary surfaces having the specific normal and tangential drop impact velocities.

4. SYMMETRIC DROP SPREADING ON MOVING SURFACES

In many practical applications such as inkjet printers, additive manufacturing, and spot soldering, symmetric spreading of drops on surfaces has a significant effect on the product quality. On the other hand, in the production lines dealing with moving surfaces having the tangential component of surface velocity, the drop impact on such surfaces leads to asymmetric drop spreading. Is it possible to achieve the symmetric drop spreading on such moving surfaces? Based on the authors' research, no studies previously addressed such a possibility. Here, using the proposed transformation framework such a possibility is investigated as follows.

In Table 3, three combined cases of drop impact on moving surfaces, which can lead to symmetric drop spreading under special conditions, are presented. Note that, these cases correspond to cases C3, C4, and C5 (in Table 2), respectively, under special conditions. In cases S1, S2, and S3, the surface velocities (in real situations) are chosen such that the tangential drop impact velocities (in transformed versions) become zero, thus, the drops impact the surfaces normally, see Table 3. Such values of surface velocity are obtained by setting the tangential drop impact velocity to zero in cases C3, C4, and C5.

However, to achieve a symmetric drop spreading, the effects of tangential gravity force (in cases S2 and S3) and induced flows due to the surface velocity (in all three cases) must be negligible. Here, to investigate such possibilities (negligible such effects), the experimental studies of (Bird et al., 2009) and (Buksh et al., 2020) are reviewed. These studies showed that the drop impact on inclined stationary surfaces or horizontal moving surfaces having tangential velocity yield identical results. Such results showed indirectly that the effects of gravity force and induced flow are negligible (within the ranges of parameters used). In both experiments, millimeter-sized drops were used and the ranges of velocities were $V_{dn} = 1.1 - 3.7\ m/s$ and $V_{dt} = 0 - 21\ m/s$ in (Bird et al., 2009) and $V_{dn} = 0.4 - 2.9\ m/s$ and $V_{dt} = 0.6 - 2.9\ m/s$ in (Buksh et al., 2020).

Table 3 Schematics of combined situations of drop impact leading to symmetric drop

Case	Real	Transformed
S1: Oblique Drop Impact on a Horizontal Moving Surface with Tangential Velocity	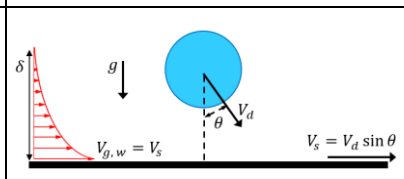	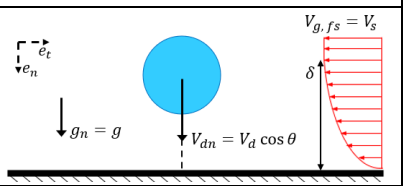
S2: Vertical Drop Impact on an Inclined Moving Surface with Tangential Downward Velocity	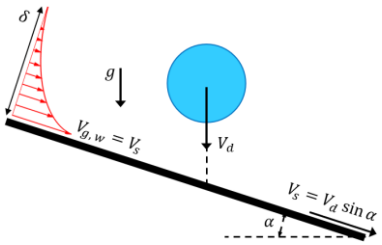	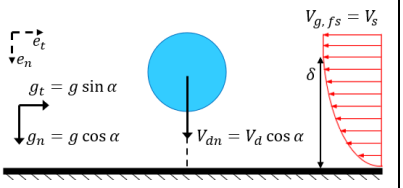
S3: Vertical Drop Impact on an Inclined Moving Surface with Horizontal Forward Velocity	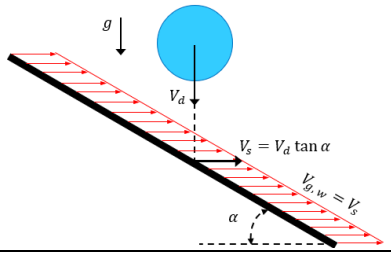	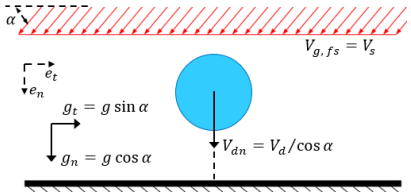

Although the drop impact situations in the experiments of (Bird et al., 2009; Buksh et al., 2020) are not the same as the cases presented in Table 3, their possible tangential gravity forces and induced flows are similar (except case S3, which have a different induced flow). This means the tangential gravity forces (in cases S2 and S3) and induced flows (in cases S1 and S2) are negligible, within the ranges of parameters used in the experiments of (Bird et al., 2009; Buksh et al., 2020). However, further investigations are needed to determine the effects of the induced flow in case S3.

Here, two technical subjects about the cases in Table 3 are discussed. First, in these cases, the surface velocity and the drop impact velocity are dependent. Second, as mentioned in section 2, providing a precise oblique drop velocity angle for case S1 (compared to a vertical drop velocity) in practice requires more equipment. However, cases S2 and S3 (having vertical drop velocities) do not require such equipment.

Therefore, when the effects of tangential gravity force and induced flows due to moving surfaces are negligible, the cases presented in Table 3 can be used for providing symmetric drop spreading. Using the moving surfaces (instead of stationary surfaces) in designing related production lines or experimental setups (where symmetric drop spreading is required) can considerably accelerate the drop impact process. Note that, in many production lines the surface velocities are not high enough to create any flow affecting drop spreading results.

5. NUMERICAL MODELING

In this section, numerical simulations are performed to evaluate some predictions of the proposed unified transformation framework under special conditions, e.g., symmetric spreading of drops on moving surfaces in cases S1 and S2 and the same asymmetric spreading of drops for cases B2, B3, and B5. For this, first our numerical methodology and code validation study are presented. Then, the simulations of six of the drop impact situations considered before (cases B1, B2, B3, and B5 in Table 1 and S1 and S2 in Table 3) are performed. At the end, the related results are analyzed and discussed.

5.1 Methodology

Here, multiphase lattice Boltzmann flux solver (MLBFS) is used for our simulations. MLBFS uses the finite volume method to solve macroscopic governing equations. However, instead of macroscopic fluxes, the corresponding mesoscopic fluxes (defined using a local lattice Boltzmann method) are evaluated at cell faces (Wang et al., 2015; Niu et al., 2018; Li et al., 2019; Yang et al., 2021; Azadi & Taeibi Rahni, 2023).

MLBFS uses Navier-Stokes (NS) and Cahn-Hilliard (CH) equations as follows:

$$\frac{\partial p}{\partial t} + \nabla.(c_s^2 \rho \vec{u}) = c_s^2 \vec{u}.\nabla\rho, \tag{1}$$

$$\frac{\partial(\rho\vec{u})}{\partial t} + \nabla.(\rho\vec{u}\vec{u}) = -\nabla p + \nabla.[\mu(\nabla\vec{u} + (\nabla\vec{u})^T)] + \vec{F}_s + \vec{F}_b, \tag{2}$$

$$\frac{\partial \phi}{\partial t} + \nabla.(\phi\vec{u}) = \nabla.\left(M\nabla\mu_\phi\right) + q, \tag{3}$$

where, c_s is speed of sound, $\vec{F}_s$ is surface tension force, and $\vec{F}_b$ is body force (e.g., gravity). In addition, ϕ is the order parameter which varies smoothly from zero (for gas) to 1 (for liquid) across the interface. Moreover, constant M is called mobility and μ_ϕ is chemical potential defined as:

$$\mu_\phi = 4A\phi(\phi-1)(\phi-0.5) - k\nabla^2\phi, \tag{4}$$

where, parameters A and k are related to surface tension coefficient (σ) and interface thickness (ξ), such that $A = 12\,\sigma/\xi$ and $k = 3\sigma\,\xi/2$. Also, $\vec{F}_s$ is given by:

$$\vec{F}_s = -\phi\nabla\mu_\phi. \tag{5}$$

Finally, source term q is used to conserve total mass of each fluid phase and is defined as:

$$q = \begin{cases} \dfrac{1}{\Delta V}\left(\dfrac{m_g^n - m_g^0}{(\rho_l - \rho_g)\,\Delta t} - \sum_{\Omega_g} M\nabla^2\mu_\phi dV\right), & 0.1 \le \phi \le 0.9, \\ 0, & elsewhere. \end{cases} \tag{6}$$

where, $0.1 \le \phi \le 0.9$ represents the interfacial region and ΔV is its volume. Moreover, Ω_g indicates gas region ($\phi \le 0.5$); m_g^n and m_g^0 are masses of gas region at $t = t^n$ and t^0; ρ_l and ρ_g are liquid and gas densities, respectively; Δt is time step; and dV is cell volume. For more details of MLBFS see (Wang et al., 2015; Niu et al., 2018; Li et al., 2019; Yang et al., 2021; Azadi & Taeibi Rahni, 2023).

5.2 Code Validation

The capability and accuracy of MLBFS for modeling different two-phase benchmark problems (e.g., 3D drop impact on flat surfaces) have been validated in several articles(Wang et al., 2015; Niu et al., 2018; Li et al., 2019; Yang et al., 2021; Azadi & Taeibi Rahni, 2023). Here, a typical 2D benchmark problem, namely: semi-circular drop deformation on a flat surface with various contact angles, is simulated to validate our code. It has an analytical solution and is close to the drop impact problem in both drop deformation and wetting boundary condition.

Initially, a stationary semi-circular drop is forced to be placed on a flat surface with contact angle of 90°. Due to interfacial forces, the drop is deformed to reach its shape and contact angle at equilibrium state. This problem is simulated using different equilibrium contact angels (30°, 60°, 90°, 120°, and 150°) leading to partial surface wetting/dewetting processes. In the absence of gravity, using the mass conservation of the drop, the equilibrium width (W_{eq}) and height (H_{eq}) of drop are derived analytically (Fakhari & Bolster, 2017) as follows:

$$\frac{W_{eq}}{D_0} = \sin(\theta_c)\sqrt{\frac{\pi}{2\theta_c - \sin(2\theta_c)}}, \qquad \frac{H_{eq}}{D_0} = \frac{1-\cos(\theta_c)}{2}\sqrt{\frac{\pi}{2\theta_c - \sin(2\theta_c)}}, \tag{7}$$

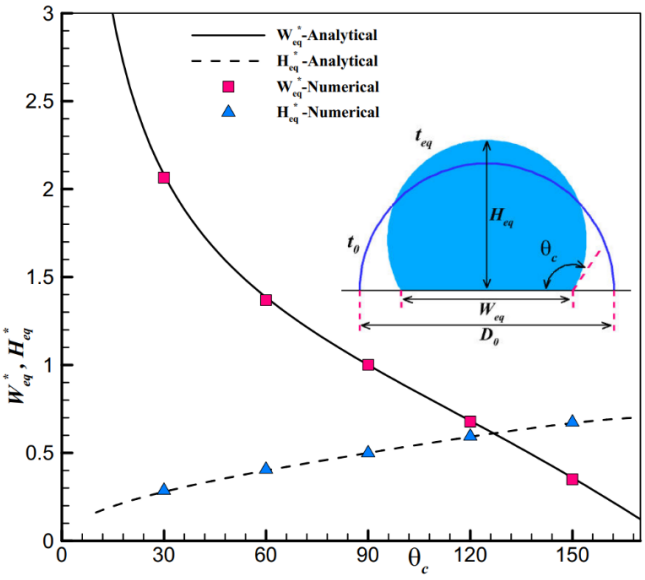

Fig. 1 Comparison of numerical values of W^*_{eq} and H^*_{eq} for different contact angles with analytical relations (7)

Table 4 Parameters used for simulation of the benchmark problem of wetting/dewetting of a semi-circular drop on a flat surface

ρ_l (kg/m^3)	μ_l $(Pa.s)$	ρ_l/ρ_g	μ_l/μ_g	σ (N/m)	D_0 (mm)
1000	0.001	843	54.2	0.0728	1

where, D_0 is the drop initial diameter and θ_c is the contact angle at equilibrium state, see drop shapes in Fig. 1.

To specify simulation parameters, the liquid and gas phases were chosen to be water and air at 15 ℃, respectively, and D_0 was set to be $1\,mm$, see Table 4. Also, a 2D rectangular domain of $3D_0 \times 1.5D_0$ with a uniform grid of 241×121 was used.

The initial distribution of order parameter (Liang et al., 2019) was set to:

$$\phi(\vec{r}) = 0.5 + 0.5\tanh\left(\frac{D_0 - 2|\vec{r} - \vec{r}_c|}{\xi}\right), \tag{8}$$

where, $\vec{r}$ is the location vector originated at the bottom left corner of the domain and $\vec{r}_c = (1.5D_0, 0)$ is the location of the drop center. Here, the interface thickness (ξ) was set to 4 grid cells (Fakhari & Bolster, 2017). Also, the initial pressure distribution was set to $p(\vec{r}) = (2\sigma/D_0)\phi$.

For boundary conditions, on the bottom surface, the no-slip boundary condition was used for NS equations and wetting boundary condition (Fakhari & Bolster, 2017) was used for CH equation as:

$$(\vec{n}.\nabla\phi)|_{wall} = -\frac{4}{\xi}\cos(\theta_c)\ \phi(1-\phi)|_{wall}, \tag{9}$$

$$(\vec{n}.\nabla\mu_\phi)\big|_{wall} = 0, \tag{10}$$

where, $\vec{n}$ is the unit normal vector of the surface. In addition, the opening (inflow/outflow) boundary condition was used for the top and side boundaries.

In Fig. 1, resulting values of dimensionless quantities $W^*_{eq} = W_{eq}/D_0$ and $H^*_{eq} = H_{eq}/D_0$ are compared with analytical relations (7), showing close agreements for all contact angles used.

5.3 Drop Impact Cases

In the following, to simulate drop impact cases, the liquid and gas phases were chosen to be water and air at 15 ℃, respectively. The values of specific parameters used are: drop diameter, $D_0 = 1\,mm$; normal drop velocity, $V_{dn} = 1\,m/s$; gravitational acceleration, $g = 9.81\,m/s^2$; and contact angle, $\theta_c = 90^\circ$. Three important dimensionless numbers in this study are: Reynolds, Weber, and Froude, as:

$$Re_n = \frac{\rho_l V_{dn} D_0}{\mu_l}, \quad We_n = \frac{\rho_l V_{dn}^2 D_0}{\sigma}, \quad Fr_n = \frac{V_{dn}^2}{gD_0}. \tag{11}$$

In Table 5, the above parameters and values of dimensionless numbers are tabulated. As shown in this table, since Fr_n^{-1} (the ratio of gravity and normal inertial forces) is less than 10^{-2}, it expects gravity force not to affect drop spreading results (García-Geijo et al., 2020), however this term has not been neglected in our simulations. Moreover, the parameters which are different, based on various drop impact cases, are presented in Table 6.

Table 5 Parameters used in all simulated drop impact cases

ρ_l (kg/m^3)	μ_l $(Pa.s)$	ρ_l/ρ_g	μ_l/μ_g	σ (N/m)	D_0 (mm)	V_{dn} (m/s)	g (m/s^2)	θ_c	Re_n	We_n	Fr_n
1000	0.001	843	54.2	0.0728	1	1	9.81	90°	1000	13.74	101.94

Table 6 Parameters which are different based on the simulated drop impact cases

Case	V_{dt} (m/s)	$V_{g,fs}$ (m/s)	g_n	g_t
B1	0	0	g	0
S1	0	-1	g	0
S2	0	-1	$g\cos 45$	$g\sin 45$
B2	1	0	g	0
B3	1	0	$g\cos 45$	$g\sin 45$
B5	1	1	g	0

As follows, the physical domain and the boundary/initial conditions used are described. A 2D rectangular domain of $L_x \times L_y = 7D_0 \times 2.7D_0$ was adopted for all our simulations. According to the boundaries of the domain (see transformed versions of the considered cases), for the bottom surface, the no-slip boundary condition was used for NS equations and the wetting boundary condition (relations (9) and (10)) was used for CH equation (Fakhari & Bolster, 2017). In addition, the opening boundary condition was used for the top boundary. The side boundaries were also considered as opening unless entering boundary layer flow exists there (see the left boundary in case B5 and the right boundary in cases S1 and S2). For such boundaries, inlet boundary condition with a second-order velocity profile of boundary layer $u_{x,bl}$ was applied as:

$$\frac{u_{x,bl}}{V_{g,fs}} = 2\left(\frac{y}{\delta}\right) - \left(\frac{y}{\delta}\right)^2, \tag{12}$$

$$\frac{\delta}{L_0} = \frac{5.477}{\sqrt{Re_{L_0}}}, \qquad Re_{L_0} = \frac{\rho_g V_{g,fs} L_0}{\mu_g}, \tag{13}$$

where, L_0 is the distance downstream from the start of the boundary layer to the start of the physical domain (Eyo et al., 2012). Here, L_0 was chosen so that $\delta = L_y$.

The order parameter distribution was initialized by relation (8) (Liang et al., 2019), where the location of drop center $\vec{r}_c = (3.5D_0, 0.5D_0)$ for cases B1, S1, and S2 (in which drop is expected to spread symmetrically) and $\vec{r}_c = (2D_0, 0.5D_0)$ for cases B2, B3, and B5 (in which drop is expected to spread asymmetrically). Here, the interface thickness (ξ) was set to 4 grid cells (Fakhari & Bolster, 2017; Liang et al., 2019). Moreover, the initial pressure distribution was set to $p(\vec{r}) = (2\sigma/D_0)\phi$ and the distribution of velocity vector was initialized by:

$$\vec{u}(\vec{r}) = \left(u_{x,bl} + (V_{dt} - u_{x,bl})\phi, -V_{dn}\phi\right), \tag{14}$$

where, $u_{x,bl}$ is given by relation (12) for cases B5, S1, and S2 (with boundary layer flow), while $u_{x,bl} = 0$ for cases B1, B2, and B3 (without initial boundary layer flow).

The dimensionless quantities $W^* = W/D_0$, $H^* = H/D_0$, and $T = t\,V_{dn}/D_0$ were used to quantify symmetric drop spreading results, where W, and H are drop spreading width and height, respectively. For asymmetric drop spreading, $UW^* = UW/D_0$ and $DW^* = DW/D_0$ were also used, where UW and DW are the corresponding upstream and downstream drop spreading widths, respectively. Note that, the boundary of the drop was defined where $\phi = 0.5$.

Table 7 Grid convergence study (case B1)

D_0 (in grid cells)	Grid	W^*_{max}	%Relative error
64	449×173	3.626	4.81
80	561×217	3.719	2.36
96	673×260	3.783	0.68
110	771×297	3.809	-

The grid convergence study was carried out using three different uniform grids for case B1 and comparing the resulting maximum drop spreading widths, see Table 7. Based on these results, the grid of 561×217 was selected for our simulations.

5.4 Results and Discussions

5.4.1 Symmetric Drop Spreading

In the following, simulation results of cases B1, S1, and S2 (in which $V_{dt} = 0$) are discussed. The resulting drop spreading shapes of these cases are presented in Table 8, wherein symmetric drop spreading is obvious for all of them. In Fig. 2, time evaluation of W^* and H^* shows very close results for all the above cases. Quantitatively at $T = 2.775$, the deviation of the wetting length of the left side of drop in cases S1 and S2 (compared to the same length in case B1) is less than 2.7% and 1.4%, respectively (are not shown here). As shown in Fig. 3, although the distributions of velocity streamlines for these cases are different, the exerting aerodynamic forces are not high enough to considerably change drop spreading shapes in cases S1 and S2.

According to these results, within the ranges of parameters used in this study, two main conclusions can be made: 1) the induced boundary layer flow due to the moving surface (in cases S1 and S2) and the tangential gravitational acceleration (in case S2) do not affect drop spreading and 2) symmetric drop spreading is also possible on moving surfaces. This interesting possibility means that for the practical applications and experimental setups, where symmetrical drop spreading is required, the surface does not need to be stationary. In such applications/setups, the use of moving surfaces (instead of stationary surfaces) can considerably accelerate the symmetric drop impact process.

5.4.2 Asymmetric Drop Spreading

In the following, the simulation results of cases B2, B3, and B5 (in which $V_{dt} \neq 0$) are discussed. The resulting drop spreading shapes of these cases are presented in Table 9, wherein the same asymmetric drop spreading shapes are obvious for all of them. In Fig. 4, time evaluation of UW^*, DW^*, and W^* shows very close results for all the above cases, quantitatively. Similarly for these three cases, the left side of drop spreads upstream until it reaches the maximum value at $T = 0.675$ and then recedes to the initial contact point and passes this point at about $T = 2.4$.

For cases B2, B3, and B5, within the ranges of parameters used in this study, the resulting identical drop spreading shapes and quantities means that the induced

Table 8 Time evolution of drop spreading shapes for the transformed versions of cases B1, S1, and S2. The dash line indicates the initial contact point of drop and surface

T	B1	S1	S2
0	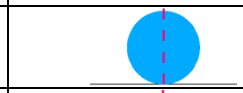	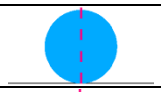	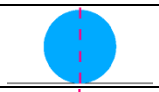
0.075		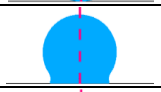	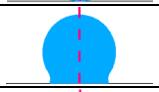
0.300	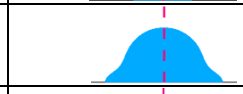	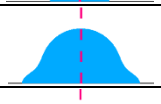	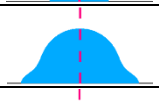
0.675	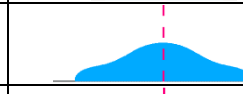	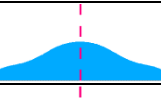	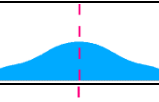
1.350		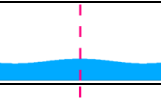	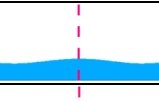
2.400	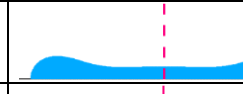		
2.775			

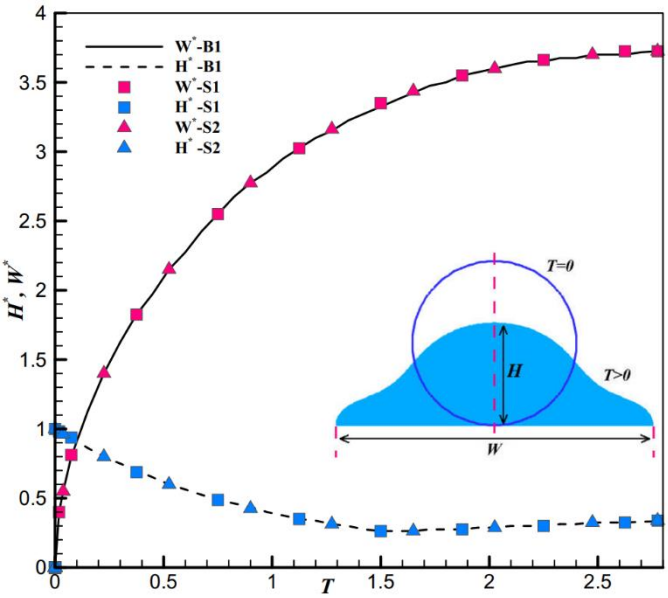

Fig. 2 Time evolution of H^* and W^* for the transformed versions of cases B1, S1, and S2

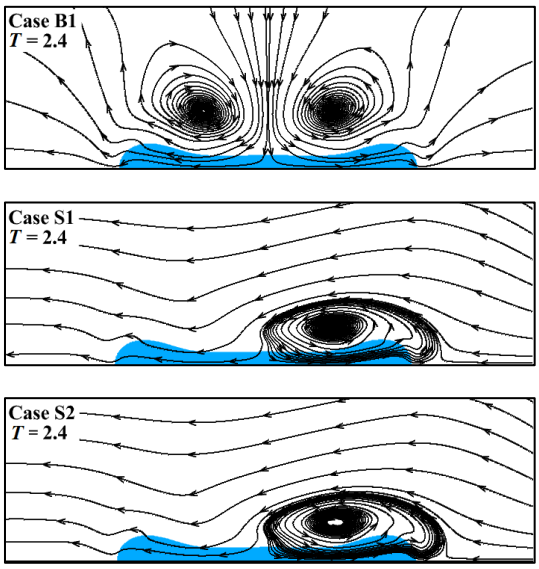

Fig. 3 Distributions of velocity streamlines for the transformed versions of cases B1, S1, and S2 at $T = 2.4$

boundary layer flow due to the moving surface (in case B5) and the tangential gravitational acceleration (in case B3) do not affect drop spreading results. Therefore, cases B2, B3, and B5 can be used interchangeably in related experimental setups and practical applications.

6. CONCLUSION AND FUTURE OUTLOOK

Due difficulties in comparing and classifying various situations of drop impact on flat surfaces, in this article the following items were performed:

- a unified transformation framework was developed to analyze, compare, and classify various situations of vertical/oblique drop impact on horizontal/inclined stationary/moving flat surfaces with/without a crossflow The use of this unified transformation framework for studying above situations significantly facilitates identification of their physical similarities/differences, as well as their technical possibilities/limitations in experimental setups and practical applications. The conditions in which some of the different situations lead to identical results and therefore can be used interchangeably were also identified (Section 2),
- the combinations of the considered basic situations of drop impact were also introduced and compared using the unified transformation framework (Section 3),

Table 9 Time evolution of drop spreading shapes for the transformed versions of cases B2, B3, and B5. The dash line indicates the initial contact point of drop and surface

T	B2 (Oblique)	B3 (Inclined)	B5 (Moving)
0	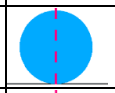	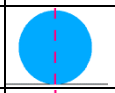	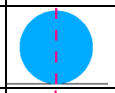
0.075	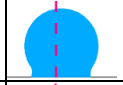	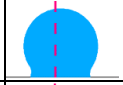	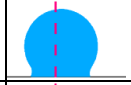
0.300			
0.675			
1.350			
2.400			
2.625			

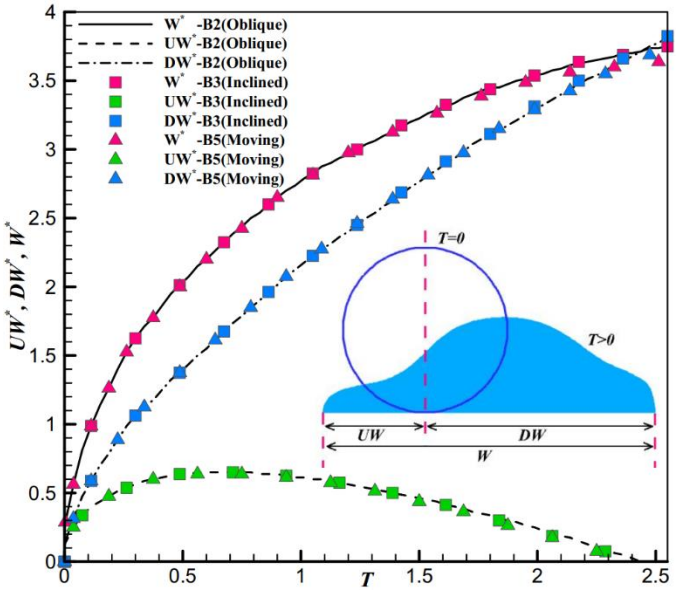

Fig. 4 Time evolution of UW^*, DW^*, and W^* for the transformed versions of cases B2, B3, and B5

- the interesting possibility of symmetrical spreading of drop on moving surfaces was investigated. Note that, the use of moving surfaces (rather than stationary ones) for design of related production lines or experimental setups (where symmetrical drop spreading is required) can considerably accelerate drop impact processes. Using the unified transformation framework, three situations of drop impact on moving surfaces (leading to symmetrical spreading) were also introduced (Section 4),
- several drop impact situations were numerically simulated. The related results well confirmed the facilitation and predictions of the proposed transformation framework (Section 5).

In this work, 2D drop impact simulations were performed and typical values of drop impact parameters were investigated. However, extension of this work can include 3D simulations and study a wide range of drop impact parameters. Obviously, the predictions of the proposed transformation framework can also be verified experimentally.

CONFLICT OF INTEREST

The authors declare that they have no conflict of interest.

AUTHORS CONTRIBUTION

Ehsan Azadi (E.A.) and Mohammad Taeibi Rahni (M.T.R.) contribution:

Conceptualization, E.A.; Methodology, E.A.; Software, E.A.; Validation, E.A. and M.T.R.; Formal Analysis, E.A. and M.T.R.; Investigation, E.A.; Project Administration, E.A. and M.T.R.; Data Curation, E.A.; Writing – Original Draft, E.A. and M.T.R.; Writing – Review & Editing, E.A. and M.T.R.; Visualization, E.A.; Supervision, M.T.R.; Project Administration, E.A. and M.T.R.; Funding Acquisition, no funding.

REFERENCES

Aboud, D. G., & Kietzig, A. M. (2015). Splashing threshold of oblique droplet impacts on surfaces of various wettability. *Langmuir*, 31(36), 10100-10111. https://doi.org/10.1021/acs.langmuir.5b02447

Aboud, D. G., & Kietzig, A. M. (2018). On the oblique impact dynamics of drops on superhydrophobic surfaces. Part I: sliding length and maximum spreading diameter. *Langmuir*, 34(34), 9879-9888. https://doi.org/10.1021/acs.langmuir.8b02034

Almohammadi, H., & Amirfazli, A. (2017a). Understanding the drop impact on moving hydrophilic and hydrophobic surfaces. *Soft Matter*, 13(10), 2040-2053. https://doi.org/10.1039/C6SM02514E

Almohammadi, H., & Amirfazli, A. (2017b). Asymmetric Spreading of a Drop upon Impact onto a Surface. *Langmuir*, 33(23), 5957-5964. https://doi.org/10.1021/acs.langmuir.7b00704

Antonini, C., Villa, F., & Marengo, M. (2014). Oblique impacts of water drops onto hydrophobic and superhydrophobic surfaces: outcomes, timing, and rebound maps. *Experiments in Fluids*, 55(4), 1-9. https://doi.org/10.1007/s00348-014-1713-9

Azadi, E., & Taeibi Rahni, M. (2023). A three-dimensional mass-conserved multiphase lattice Boltzmann flux solver for incompressible flows with large density and viscosity ratios. *Accepted to be Published by Advances in Applied Mathematics and Mechanics*.

Benther, J. D., Pelaez-Restrepo, J. D., Stanley, C., & Rosengarten, G. (2021). Heat transfer during multiple droplet impingement and spray cooling: Review and prospects for enhanced surfaces. *International Journal of Heat and Mass Transfer*, 178, 121587. https://doi.org/10.1016/j.ijheatmasstransfer.2021.121587

Bird, J. C., Tsai, S. S., & Stone, H. A. (2009). Inclined to splash: triggering and inhibiting a splash with tangential velocity. *New Journal of Physics*, 11(6), 063017. https://doi.org/10.1088/1367-2630/11/6/063017

Buksh, S., Almohammadi, H., Marengo, M., & Amirfazli, A. (2019). Spreading of low-viscous liquids on a stationary and a moving surface. *Experiments in Fluids*, 60(4), 1-12. https://doi.org/10.1007/s00348-019-2715-4

Buksh, S., Marengo, M., & Amirfazli, A. (2020). Impacting of droplets on moving surface and inclined surfaces. *Atomization and Sprays*, 30(8). https://doi.org/10.1615/AtomizSpr.2020033015

Carrolo, G., Ribeiro, D., Barata, J. M., & Silva, A. R. (2019). *Aerodynamic breakup of a single droplet due to a crossflowed airstream*. AIAA Scitech 2019 Forum, 0628. https://doi.org/10.2514/6.2019-0628

Chen, R. H., & Wang, H. W. (2005). Effects of tangential speed on low-normal-speed liquid drop impact on a non-wettable solid surface. *Experiments in Fluids*, 39(4), 754-760. https://doi.org/10.1007/s00348-005-0008-6

Cimpeanu, R., & Papageorgiou, D. T. (2018). Three-dimensional high speed drop impact onto solid surfaces at arbitrary angles. *International Journal of Multiphase Flow*, 107, 192-207. https://doi.org/10.1016/j.ijmultiphaseflow.2018.06.011

Cui, J., Chen, X., Wang, F., Gong, X., & Yu, Z. (2009). Study of liquid droplets impact on dry inclined surface. *Asia-Pacific Journal of Chemical Engineering*, 4(5), 643-648. https://doi.org/10.1002/apj.309

Cunha, N., Ribeiro, D., Barata, J. M., & Silva, A. R. (2018). *The splash deposition transition limits of a biofuel droplet wall impact with a and without crossflow*. 14th International Conference on Liquid Atomization and Spray Systems 2020. ILASS Europe, Institute for Liquid Atomization and Spray Systems. ICLASS 2018-14th International Conference on Liquid Atomization and Spray Systems 2020. ILASS Europe, Institute for Liquid Atomization and Spray Systems. Retrieved from http://hdl.handle.net/10400.6/12166

Dai, B., Liu, C., Liu, S., Wang, D., Wang, Q., Zou, T., & Zhou, X. (2023). Life cycle techno-enviro-economic assessment of dual-temperature evaporation transcritical CO2 high-temperature heat pump systems for industrial waste heat recovery. *Applied Thermal Engineering*, 219, 119570. https://doi.org/10.1016/j.applthermaleng.2022.119570

Eyo, A. E., Ogbonna, N., & Ekpenyong, M. E. (2012). Comparison of the exact and approximate values of certain parameters in laminar boundary layer flow using some velocity profiles. *Journal of Mathematics Research*, 4(5), 17. https://doi.org/10.5539/jmr.v4n5p17

Fakhari, A., & Bolster, D. (2017). Diffuse interface modeling of three-phase contact line dynamics on curved boundaries: A lattice Boltzmann model for large density and viscosity ratios. *Journal of Computational Physics*, 334, 620-638. https://doi.org/10.1016/j.jcp.2017.01.025

Fathi, S., Dickens, P., & Fouchal, F. (2010). Regimes of droplet train impact on a moving surface in an

additive manufacturing process. *Journal of Materials Processing Technology*, 210(3), 550-559. https://doi.org/10.1016/j.jmatprotec.2009.10.018

Ferrao, I., Ribeiro, D., Barata, J. M., & Silva, A. R. (2019). *Comparative study of droplet impact onto sloped surface versus a droplet impact onto a surface with a crossflow*. AIAA Scitech 2019 Forum, 0629. https://doi.org/10.2514/6.2019-0629

Ferrao, I., Vasconcelos, D., Ribeiro, D., Silva, A., & Barata, J. (2020). A study of droplet deformation: The effect of crossflow velocity on jet fuel and biofuel droplets impinging onto a dry smooth surface. *Fuel*, 279, 118321. https://doi.org/10.1016/j.fuel.2020.118321

García-Geijo, P., Riboux, G., & Gordillo, J. M. (2020). Inclined impact of drops. *Journal of Fluid Mechanics*, 897, A12-46. https://doi.org/10.1017/jfm.2020.373

Gordillo, J. M., Riboux, G., & Quintero, E. S. (2019). A theory on the spreading of impacting droplets. *Journal of Fluid Mechanics*, 866, 298-315. https://doi.org/10.1017/jfm.2019.117

Hao, J., & Green, S. I. (2017). Splash threshold of a droplet impacting a moving substrate. *Physics of Fluids*, 29(1), 012103. https://doi.org/10.1063/1.4972976

Hao, J., Lu, J., Lee, L., Wu, Z., Hu, G., & Floryan, J. M. (2019). Droplet splashing on an inclined surface. *Physical Review Letters*, 122(5), 054501. https://doi.org/10.1103/PhysRevLett.122.054501

Jiang, M., & Zhou, B. (2020). Droplet behaviors on inclined surfaces with dynamic contact angle. *International Journal of Hydrogen Energy*, 45(54), 29848-29860. https://doi.org/10.1016/j.ijhydene.2019.07.173

Josserand, C., & Thoroddsen, S. T. (2016). Drop impact on a solid surface. *Annual Review of Fluid Mechanics*, 48(1), 365-391. https://doi.org/10.1146/annurev-fluid-122414-034401

LeClear, S., LeClear, J., Park, K. C., & Choi, W. (2016). Drop impact on inclined superhydrophobic surfaces. *Journal of Colloid and Interface Science*, 461, 114-121. https://doi.org/10.1016/j.jcis.2015.09.026

Li, H. (2013). Drop impact on dry surfaces with phase change. [Doctoral Thesis, Mechanical Engineering, Technische Universität Darmstadt: Darmstadt]. Retrieved from https://tuprints.ulb.tu-darmstadt.de/id/eprint/3550

Li, Y., Niu, X. D., Wang, Y., Khan, A., & Li, Q. Z. (2019). An interfacial lattice Boltzmann flux solver for simulation of multiphase flows at large density ratio. *International Journal of Multiphase Flow*, 116, 100-112. https://doi.org/10.1016/j.ijmultiphaseflow.2019.04.006

Liang, H., Liu, H., Chai, Z., & Shi, B. (2019). Lattice Boltzmann method for contact-line motion of binary fluids with high density ratio. *Physical Review E*, 99(6), 063306. https://doi.org/10.1103/PhysRevE.99.063306

Lunkad, S. F., Buwa, V. V., & Nigam, K. P. (2007). Numerical simulations of drop impact and spreading on horizontal and inclined surfaces. *Chemical Engineering Science*, 62(24), 7214-7224. https://doi.org/10.1016/j.ces.2007.07.036

Marengo, M., Antonini, C., Roisman, I. V., & Tropea, C. (2011). Drop collisions with simple and complex surfaces. *Current Opinion in Colloid & Interface Science*, 16(4), 292-302. https://doi.org/10.1016/j.cocis.2011.06.009

Mohammad Karim, A. (2023). Physics of droplet impact on various substrates and its current advancements in interfacial science: A review. Journal of Applied Physics, 133(3). https://doi.org/10.1063/5.0130043

Moreira, A. N., Moita, A. S., & Panao, M. R. (2010). Advances and challenges in explaining fuel spray impingement: How much of single droplet impact research is useful? *Progress in Energy and Combustion Science*, 36(5), 554-580. https://doi.org/10.1016/j.pecs.2010.01.002

Niu, X. D., Li, Y., Ma, Y. R., Chen, M. F., Li, X., & Li, Q. Z. (2018). A mass-conserving multiphase lattice Boltzmann model for simulation of multiphase flows. *Physics of Fluids*, 30(1), 013302. https://doi.org/10.1063/1.5004724

Pasandideh-Fard, M., Bhola, R., Chandra, S., & Mostaghimi, J. (1998). Deposition of tin droplets on a steel plate: simulations and experiments. *International Journal of Heat and Mass Transfer*, 41(19), 2929-2945. https://doi.org/10.1016/S0017-9310(98)00023-4

Pasandideh-Fard, M., Qiao, Y. M., Chandra, S., & Mostaghimi, J. (1996). Capillary effects during droplet impact on a solid surface. *Physics of Fluids*, 8(3), 650-659. https://doi.org/10.1063/1.868850

Pereira, F. L. (2019). *Effect of crossflow variation on impacting droplets.* [Doctoral dissertation, Universidade da Beira Interior]. Portugal.

Raman, K. A. (2019). Normal and oblique droplet impingement dynamics on moving dry walls. *Physical Review E*, 99(5), 053108. https://doi.org/10.1103/PhysRevE.99.053108

Rioboo, R., Tropea, C., & Marengo, M. (2001). Outcomes from a drop impact on solid surfaces. *Atomization and Sprays*, 11(2). https://doi.org/10.1615/AtomizSpr.v11.i2.40

Sahoo, N., Khurana, G., Harikrishnan, A. R., Samanta, D., & Dhar, P. (2020). Post impact droplet hydrodynamics on inclined planes of variant wettabilities. *European Journal of Mechanics-*

B/Fluids, 79, 27-37. https://doi.org/10.1016/j.euromechflu.2019.08.013

Shen, C., Yu, C., & Chen, Y. (2016). Spreading dynamics of droplet on an inclined surface. *Theoretical and Computational Fluid Dynamics*, 30(3), 237-252. https://doi.org/10.1007/s00162-015-0377-2

Shusheng, Z., Hao, L., Li-Zhi, Z., Saffa, R., Zafer, U., & Huaguan, Z. (2020). A lattice Boltzmann simulation of oblique impact of a single rain droplet on super-hydrophobic surface with randomly distributed rough structures. *International Journal of Low-Carbon Technologies*, 15(3), 443-449. https://doi.org/10.1093/ijlct/ctaa004

Šikalo, Š., Tropea, C., & Ganić, E. N. (2005). Impact of droplets onto inclined surfaces. *Journal of Colloid and Interface Science*, 286(2), 661-669. https://doi.org/10.1016/j.jcis.2005.01.050

Wang, X., Xu, B., Chen, Z., Del Col, D., Li, D., Zhang, L., & Cao, Q. (2022). Review of droplet dynamics and dropwise condensation enhancement: Theory, experiments and applications. *Advances in Colloid and Interface Science*, 102684. https://doi.org/10.1016/j.cis.2022.102684

Wang, Y., Shu, C., & Yang, L. M. (2015). An improved multiphase lattice Boltzmann flux solver for three-dimensional flows with large density ratio and high Reynolds number. *Journal of Computational Physics*, 302, 41-58. https://doi.org/10.1016/j.jcp.2015.08.049

Xu, L. (2007). Liquid drop splashing on smooth, rough, and textured surfaces. *Physical Review E*, 75(5), 056316. https://doi.org/10.1103/PhysRevE.75.056316

Xu, L., Zhang,, W. W., & Nagel, S. R. (2005). Drop splashing on a dry smooth surface. *Physical Review Letters*, 94(18), 184505. https://doi.org/10.1103/PhysRevLett.94.184505

Xu, M., Zhang, J., & Chen, R. (2022). Cooling effect of droplet impacting on heated solid surface. *International Journal of Heat and Mass Transfer*, 183, 122070. https://doi.org/10.1016/j.ijheatmasstransfer.2021.122070

Yang, L., Shu, C., Chen, Z., Wang, Y., & Hou, G. (2021). A simplified lattice Boltzmann flux solver for multiphase flows with large density ratio. *International Journal for Numerical Methods in Fluids*, 93(6), 1895-1912. https://doi.org/10.1002/fld.4958

Yin, C., Wang, T., Che, Z., Jia, M., & Sun, K. (2018). Oblique impact of droplets on microstructured superhydrophobic surfaces. *International Journal of Heat and Mass Transfer*, 123, 693-704. https://doi.org/10.1016/j.ijheatmasstransfer.2018.02.060

Zen, T. S., Chou, F. C., & Ma, J. L. (2010). Ethanol drop impact on an inclined moving surface. *International Communications in Heat and Mass Transfer*, 38(8), 1025-1030. https://doi.org/10.1016/j.icheatmasstransfer.2010.05.003

Zhan, H., Lu, C., Liu, C., Wang, Z., Lv, C., & Liu, Y. (2021). Horizontal motion of a superhydrophobic substrate affects the drop bouncing dynamics. *Physical Review Letters*, 126(23), 234503. https://doi.org/10.1103/PhysRevLett.126.234503

Zhang, R., Hao, P., & He, F. (2017). Drop impact on oblique superhydrophobic surfaces with two-tier roughness. *Langmuir*, 33(14), 3556-3567. https://doi.org/10.1021/acs.langmuir.7b00569

Zhao, H., Han, X., Li, J., Li, W., Huang, T., Yu, P., & Wang, L. (2022). Numerical investigation of a droplet impacting obliquely on a horizontal solid surface. *Physical Review Fluids*, 7(1), 013601. https://doi.org/10.1103/PhysRevFluids.7.013601